In-vivo Quantitative Depth Measurement of the Human Gingival Sulcus Based on Interferometry System with Detection Algorithm

Hoseong Cho, Jaeyul Lee, Jaewon Song, Mansik Jeon*, and Jeehyun Kim
School of Electronics Engineering, College of IT Engineering, Kyungpook National University, Daegu, Republic of Korea
Email: ghtjd419@knu.ac.kr, jaeyul@knu.ac.kr, jwsong@knu.ac.kr, mansikjeon@gmail.com*, jeehk@knu.ac.kr

***Abstract*—Optical coherence tomography (OCT) has magnetized substantial notice in biomedical optical imaging since it can reveal the inner structures. Gingival is a soft tissue that surrounds a tooth. In dentistry, the depth of the gingival sulcus reveals clinical diagnostic criteria for periodontal tissue status. We propose an algorithm for measuring the gingival sulcus in the OCT 2D cross-sectional images and verified the algorithm using OCT systems with three different wavelength bands. Periodontal tissues of six healthy individuals, among them maxillary and mandibular incisors and posteriors, were taken. We have obtained a clear comparison of quantitative and qualitative measurements, and to evaluate gingival sulcus non-destructively. Additionally, commercial Sobel and Canny operators primarily used, were compared with the proposed algorithm to confirm reducing sensitivity to noise and speckle in OCT images.**

***Index Terms*— Detection algorithms, biomedical optical imaging, optical coherence tomography**

I. Introduction

Gingival is a soft tissue that surrounds a tooth. In dentistry, the depth of the gingival sulcus reveals clinical diagnostic criteria for periodontal tissue status [1]. The manual probe is the standard gold method commonly used [2, 3]. However, manual probing techniques generally cause pain to the patient. It may also cause periodontal bleeding during diagnosis. To rectify the human errors in manual probing, therefore, an automatic probe was developed. This mechanical probe can keep the prod force constant during measure the depth. However, according to the patient, it is hard to work and makes the patient even more uncomfortable [4]. To alleviate the inconvenience, imaging technology such as computed tomography (CT) [5, 6], magnetic resonance imaging (MRI) [7], ultrasonic imaging [8], and optical imaging technology has been used. These techniques suffer from slow shooting speeds and low resolution.

In particular, optical coherence tomography (OCT) has been attracting much attention for the use of diagnostic methods because it can realize real-time non-invasive 2D cross-sectional images [9]. OCT also has been studied to the measurement of gingival sulcus with small animal models, medium animals, and clinical trials [10-13]. Previous studies have shown the usefulness of Sobel and Canny edge operators for improving the accuracy of measuring gingival sulcus [14]. However, this operator is very sensitive to signals in OCT images, such as noise and speckle changes, not only to detect the desired location.

We propose an algorithm based on intensity mean difference, in this study, to reveal gingival sulcus in OCT images. We utilized two commercially-available swept-source OCT systems (1310 nm and 1060 nm) and laboratory-customized spectral-domain OCT system (840 nm) to verify the proposed algorithm. The images were processed using three algorithms (Canny, Sobel, and intensity mean difference).

II. Experimental setup and Method

A. In Vivo Preparation of Human Gingival Sulcus

In vivo images of human periodontal tissues were taken in every pair of maxillary central incisors, mandibular central incisors, and later incisors with every six participants (total 36 teeth). Also, we arbitrarily named T1-T6. All the human experiments were performed following the guidelines of the Institutional Animal and Human Care and Use Committee of Kyungpook National University (No. 2017-0145-1). To get accurate dimensions, you need to divide the OCT scale by the refractive index of the relevant tissue area, (such as n=1.3 for oral mucosa, n=1.6 for enamel and gum, n=1.5 for dentin, and n=1.4 for gingival sulcus). This is because the amount of backscattered light in dense media decreases exponentially with depth, resulting in compression of the axial image. Hence, we use 1.41 ± 0.06 as the refractive index of gingival tissue in this study, which revealed in previous literature studies. The above mentioned refractive index precisely confirmed, further, the applicability for the wavelength bands, between 850 nm ~ 1325 nm.

Manuscript received April 5, 2019; revised March 9, 2020.

doi: 10.18178/ijmerr.9.5.771-774

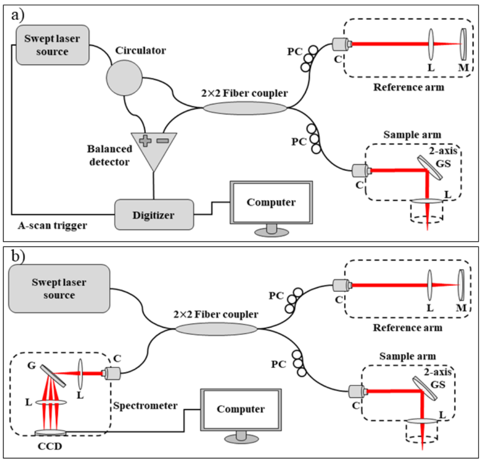

Figure 1. Schematic diagram of OCT systems. a) The schematic diagram for SS-OCT. b) The schematic diagram for SD-OCT. C: collimator; L: lens; M: mirror; PC: polarization controller; GS: Galvano scanner, G: Grating, CCD: Charge-Coupled Device.

B. *OCT System Configuration*

Two swept-source OCT systems (SS-OCT) and a spectral-domain OCT (SD-OCT) system used. The schematic diagram shows in Fig. 1. The utilized SS-OCT systems were commercial OCT systems (Thorlabs. Inc, OCS1310V1 and Santec. Inc, IVS-2000). The Thorlabs system consists of center wavelength at 1310 nm with a spectral bandwidth of > 97 nm. The system swept rate was 100 kHz with an axial and transverse resolution 16 µm and 25 µm in the air. The Santec system consists of center wavelength at 1060 nm with a spectral bandwidth of > 100 nm. The swept-source swept rate was 100 kHz with an axial resolution 18 µm and a transverse resolution of 15 µm in the air. A customized SD-OCT system centered at 840 nm with a 3-dB bandwidth of 50 nm. The axial scan rate of the system was 70 kHz with an axial and transverse resolution 10 µm and 11 µm in the air.

C. *Image Processing Algorithm*

The proposed detection algorithm starts with loading the OCT image and examines the condition in every pixel, shown in Fig. 2. The algorithm works two processes, verifying vertical and horizontal linearity. N by M pixel size window is selected in the horizontal linearity verifying process so that the target pixel is in the center. After that, the pixel window is split into two sub-pixel windows (top and bottom) with the center row superimposed, including the target pixel. The values of all the pixels in each sub-window averaged. The difference between the average intensities of the two sub-windows, calculated as absolute values, is estimated. Then compare this absolute value with a predefined value and verify the linearity (indicated by 1 or 0)—the same process executed in the vertical direction. Then the target pixel is moved until all pixels executed. If the final boundary detected the OCT image does not reveal the gingival sulcus, the predefined threshold value can be changed.

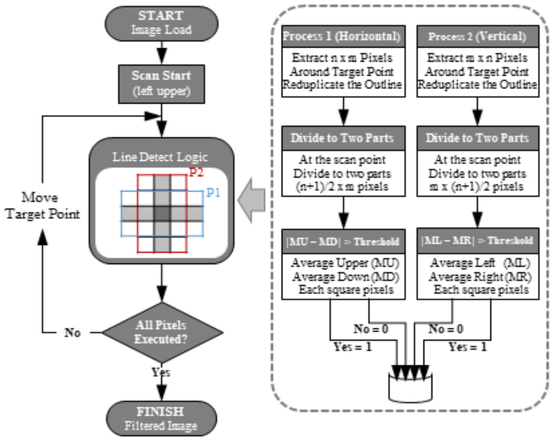

Figure 2. The flow chart of the OCT-Pixel intensity-dependent image processing algorithm.

III. Results and Discussion

We evaluated the efficacy of the proposed edge detection algorithm and compared it to Canny and Sobel, which are edge detection algorithms that mainly used. Fig. 3 shows the final edge detection image executed by Canny, Sobel, and the intensity mean difference algorithm. On closer examination, it appears that Sobel edge detection algorithms have too high a sensitivity to speckle noise. Moreover, Canny edge detection algorithms have linear distortions in OCT images. Compared with the two algorithms, it showed that the presented algorithm is accurate.

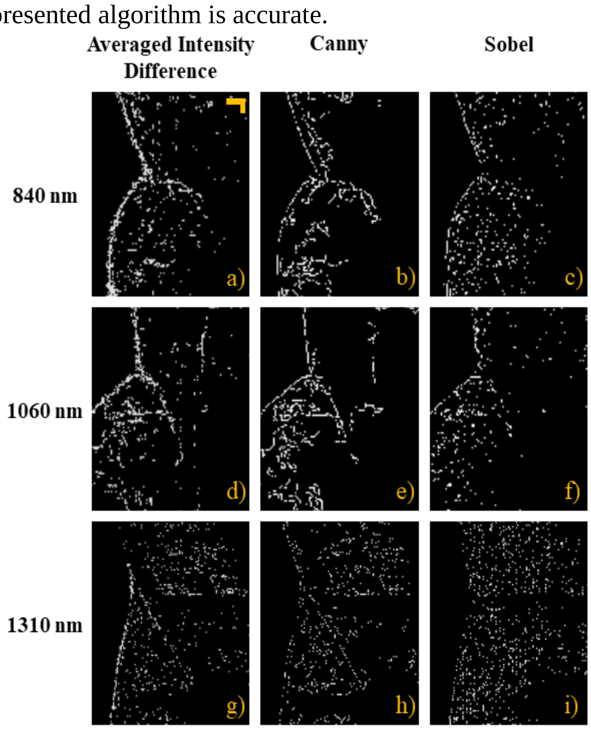

Figure 3. Images after image processing. (a-c) images are analysis results of the 840 nm wavelength image; (d-f) are analysis results of the 1060 nm image; (g-i) are analysis results of the 1310 nm image; scale bar in (a) is 200 µm.

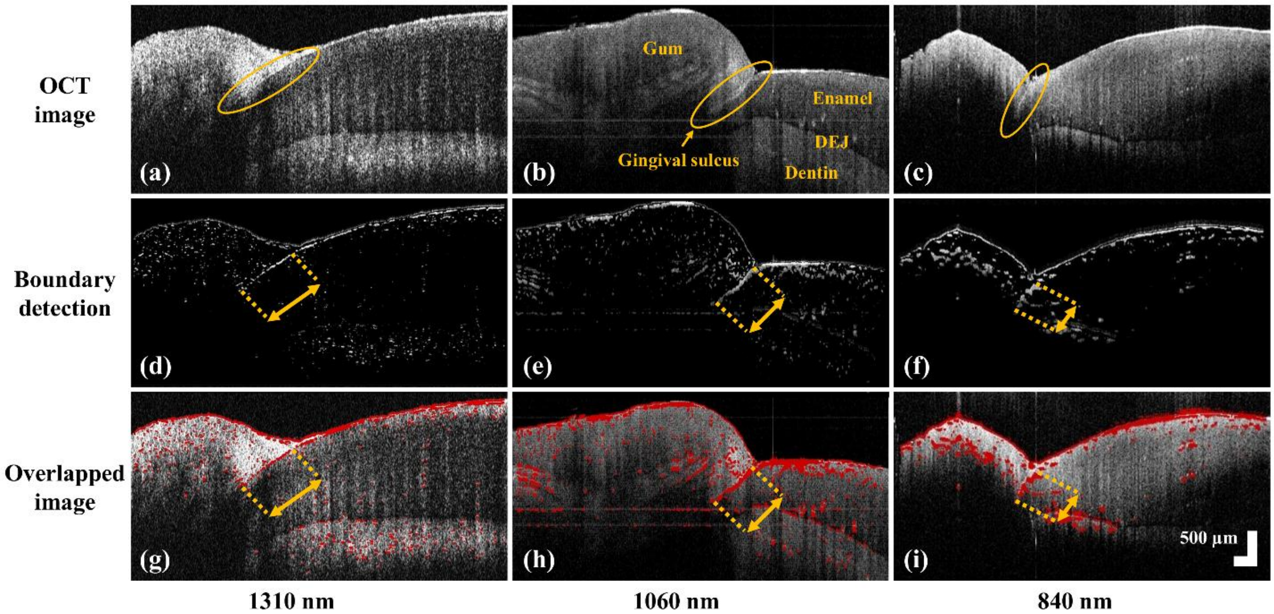

Figure 4. Images of measuring gingival sulcus using image processing. (a), (d), and (g) are analysis results of the 1310 nm wavelength image; (b), (e), and (h) are analysis results of the 1060 nm image; (c), (f), and (i) are analysis results of the 840 nm image. DEJ: dentin-enamel junction.

We quantitatively measured the depth of the gingival sulcus by boundary detection using an image processing method. In Fig. 4(a)-(c), OCT images reveal the structures including the gingival sulcus. However, the gingival sulcus depth was not different in the near gingiva region. After the boundary detection by image processing, the sulcus was distinguished more clearly, as shown in Fig. 4(d)-(f). Thus, we were able to more clearly measure the depth of the gingival sulcus with superimposed images using the edge detection of OCT images, as shown in Fig. 4 (g)-(i).

To improve the accuracy of depth information, imaging experiments were performed on every three regions of interest in all in vivo tooth samples and then measured three times for each image. In other words, the proposed algorithm applied in 324 OCT images (108 images in each system). Also, the below values are the mean value measured by each OCT system. The sulcus depths measured by the three different wavelength-based OCT system in the maxilla region were 1,002 ± 282 µm (1310 nm), 883 ± 251 µm (1060 nm), and 383 ± 130 µm (840 nm). Moreover, in the mandible, 892 ± 297 µm (1310 nm), 774 ± 241 µm (1060 nm), and 577 ± 169 µm (840 nm) depths measured.

IV. Conclusions

We analyzed the depth of the gingival sulcus and compared them with each other using three different wavelength-based OCT systems with a central wavelength of 1310 nm, 1060 nm, and 840 nm, respectively. The primary intention of this pilot study was to compare qualitative and quantitative representations of gingival sulcus between multiple wavelengths bands-based OCT systems using the proposed algorithm. Invasive standard gold methods can measure more deep regions of the gingival sulcus. However, the pilot study reveals that the intensity mean difference algorithm with the OCT system is capable of acquiring morphological and quantitative information with a sufficient depth range. However, the application of 840 nm, 1060 nm, and 1310 nm OCT system limits the inspection of the inner tooth specimens. If it can replace a hand-held OCT inspection probe integrated, it is possible to fix up the limitations about the inner tooth image acquisition. In summary, qualitative and quantitative measurements of gingival sulcus obtained by the intensity mean difference algorithm provides a reliable platform and can be used as threshold information for real-time surveying applications that measure depth.

Conflict of Interest

"The authors declare no conflict of interest".

Author Contributions

Hoseong Cho and Jaeyul Lee conducted the research; Jaewon Song, Mansik Jeon, and Jeehyun Kim analyzed the data; Hoseong Cho wrote the paper; all authors had approved the final version.

Acknowledgment

This research was supported by the National Research Foundation of Korea (NRF) grant funded by the Korea government, MSIT (No. 2018R1A5A1025137) and by the Bio & Medical Technology Development Program of the NRF funded by the Korean government, MSIP(2017M3A9E2065282).

REFERENCES

[1] B. W. Colston, M. J. Everett, L. B. D. Silva, L. L. Otis, P. Stroeve, and H. Nathel, "Imaging of hard- and soft-tissue structure in the oral cavity by optical coherence tomography," *Applied Optics*, vol 37, pp. 3582-3585, 1998.

[2] U. Velden, "Errors in the assessment of pocket depth in vitro," *Journal of Clinical Periodontology*. vol. 5, pp. 182-187, 1978.

[3] M. A. Listgarten, "Periodontal probing: What does it mean?" *Journal of Clinical Periodontology*, vol. 7, pp. 165-176, 1980.

[4] L. O. Fernandes, C. C. Mota, L. S. Melo, Costa Soares, M. U., Silva Feitosa, D. and A. S. Gomes, "In vivo assessment of periodontal structures and measurement of gingival sulcus with optical coherence tomography: A pilot study," *Journal of Biophotonics*. vol. 10, pp. 862-869, 2017.

[5] A. L. Janu áRio, M. Barriviera, and W. R. Duarte, "Soft tissue cone-beam computed tomography: A novel method for the measurement of gingival tissue and the dimensions of the dentogingival unit," *Journal of Esthetic and Restorative Dentistry*. vol. 20, pp. 366-373, 2008.

[6] B. Weidmann, P. Sahrmann, A. Bindl, M. Roos, P. R. Schmidlin, "Depth determination of artificial periodontal pockets using cone-beam tomography and radio-opaque material: an in vitro feasibility study," *Swiss Dental Journal*, vol. 124, no. 4, pp. 406-415, 2014.

[7] R. Schara, I. Serša, and U. Skalerič, "T1 relaxation time and magnetic resonance imaging of inflamed gingival tissue," *Dentomaxillofacial Radiology*., vol. 38, no. 4, pp. 216-223, 2009.

[8] T. Eger, H. Müller, and A. Heinecke, "Ultrasonic determination of gingival thickness," *Journal of Clinical Periodontology*, vol. 23, pp. 839-845, 1996.

[9] H. Schneider, K. J. Park, M. Häfer, Rüger C, Schmalz G, Krause F, Schmidt J, Ziebolz D, Haak R., "Dental applications of optical coherence tomography (OCT) in cariology," *Applied Sciences*. vol. 7, no. 5, 472, 2017.

[10] L. O. Fernandes, C. C. B. O. Mota, L. S. A. de Melo, M. U. S. da Costa Soares, D. da Silva Feitosa, and A. S. L. Gomes, "In vivo assessment of periodontal structures and measurement of gingival sulcus with optical coherence tomography: A pilot study," *J. Biophoton.*, vol. 10, nos. 6_7, pp. 862-869, 2017.

[11] C. C. B. O. Mota, L. O. Fernandes, R. Cimões, and A. S. L. Gomes, "Noninvasive periodontal probing through Fourier-domain optical coherence tomography," *J. Periodontology*, vol. 86, no. 3, pp. 1087-1094, 2015.

[12] S. Kakizaki, A. Aoki, M. Tsubokawa, T. Lin, K. Mizutani, G. Koshy, A. Sadr, S. Oda, Y. Sumi, and Y. Izumi, "Observation and determination of periodontal tissue pro_le using optical coherence tomography," *J. Periodontal Res.*, vol. 53, no. 2, pp. 188-199, 2018.

[13] S. R. Kang, J. M. Kim, S. H. Kim, H. J. Park, T. I. Kim, and W. J. Yi, "Tooth cracks detection and gingival sulcus depth measurement using optical coherence tomography," in *Proc. IEEE 39th Annu. Int. Conf. Eng. Med. Biol. Soc. (EMBC)*, Jul. 2017, pp. 4403-4406.

[14] S. H. Kim, S. R. Kang, H. J. Park, J. M. Kim, W. J. Yi, and T. I. Kim, "Improved accuracy in periodontal pocket depth measurement using optical coherence tomography," *J. Periodontal Implant Sci.*, vol. 47, no. 1, pp. 13-19, 2017.

Hoseong Cho is currently doing his B.Sc in Electronics Engineering in Kyungpook National University, Daegu, Republic of Korea. His research interest is in image processing and analysis biomedical imaging techniques.

Jaeyul Lee is currently pursuing the Ph.D. degree with the School of Electronics Engineering, Kyungpook National University, Daegu, South Korea. His research background includes optical imaging techniques, photoacoustic microscopy, optical coherence tomography, and handheld instruments for optimization of the optical coherence tomography and photoacoustic microscopy system.

Jaewon Song received the Ph.D. degree in electrical and electronics engineering from the Korea Advanced Institute of Science and Technology, Daejeon, South Korea, in 1984. He is currently a Full Professor with the School of Electronics Engineering, Kyungpook National University. His research interests are in the development of optical communication and integrated optics.

Mansik Jeon received the Ph.D. degree in electronics engineering from Kyungpook National University, Daegu, South Korea, in 2011. He is currently as Assistant Professor with the School of Electronics Engineering, Kyungpook National University. His research interests are in the development of nonionizing and noninvasive novel biomedical imaging techniques, including photoacoustic tomography, photoacoustic microscopy, optical coherence tomography, ultrasonic imaging, handheld scanner, and their clinical applications.

Jeehyun Kim received the Ph.D. degree in biomedical engineering from the University of Texas at Austin, USA, in 2004. He was a Post-Doctoral Researcher with the Beckman Laser Institute, University of California at Irvine. He is currently a Full Professor with Kyungpook National University, Daegu, South Korea. His research interest is in biomedical imaging and sensing, neuroscience studies using multiphoton microscopy, photo-acoustic imaging, and other novel applications of sensors.